THE JOURNAL OF PHYSICAL CHEMISTRY LETTERS
A JOURNAL OF THE AMERICAN CHEMICAL SOCIETY

pubs.acs.org/JPCL Letter

Nanochemistry in the Gas Phase: Coulombic Adducts of Atomically Precise Noble Metal Nanoclusters and Their Concomitant Reactions

Swetashree Acharya, Seth Adam Horn, Vikash Khokhar, Nicolas J. Pizzala, Vivek Yadav, Subrata Duary, Tomas Base,* De-en Jiang,* Scott A. McLuckey,* and Thalappil Pradeep*

Cite This: https://doi.org/10.1021/acs.jpclett.6c00072 Read Online

ACCESS | Metrics & More | Article Recommendations | Supporting Information

ABSTRACT: In this study, we explore for the first time interactions of atomically precise noble metal nanoclusters (NCs) in the gas phase, revealing fundamental nanoscale reactivity beyond solvent effects. Using ion-selected mass spectrometry and theoretical calculations, we investigate and establish the formation of a Coulombic ion pair between two oppositely charged NC ions, $[Ag_{17}(o_1\text{-CBT})_{12}]^{3-}$ (o_1-CBT = ortho-1-carboranethiol) and $[Cu_{14}(o_{9,12}\text{-CBDT})_6]^{+}$ ($o_{9,12}$-CBDT = ortho-9,12-carboranedithiol), that undergo metal exchange to form alloy NCs, focusing on how atom exchange processes can be understood in the isolated gas phase. The Coulombic contribution to the binding energy of the NC ion pair was estimated to be ∼66%, while the rest was from intercluster ligand interaction through van der Waals forces. Similar behavior across diverse oppositely charged NC ion pairs, including $[Ag_{29}(1,3\text{-BDT})_{12}]^{3-}$ (1,3-BDT = 1,3-benzenedithiol), $[PdAg_{28}(1,3\text{-BDT})_{12}]^{4-}$, $[PtAg_{28}(1,3\text{-BDT})_{12}]^{4-}$, $[Ag_{13}Cu_4(o_1\text{-CBT})_{12}]^{3-}$, $[Au_{25}(2\text{-PET})_{18}]^{-}$ (2-PET = 2-phenylethanethiol), $[PdAg_{24}(2,4\text{-DMBT})_{18}]^{2-}$ (2,4-DMBT = 2,4-dimethylbenzenethiol), $[PtAg_{24}(2,4\text{-DMBT})_{18}]^{2-}$, $[Cu_{14}(o_{9,12}\text{-CBDT})_6]^{+}$, $[Ag_{21}(m_9\text{-CBT})_{12}]^{+}$ (m_9-CBT = meta-9-carboranethiol), and $[Ag_{22}(2,5\text{-DMBT})_{12}Cl_4(DPPB)_4]^{+}$ (DPPB= diphenylphosphenobutane), confirms the universality of this process. Dithiol ligand exchange was observed between $[Ag_{29}(1,3\text{-BDT})_{12}]^{3-}$ and $[Cu_{14}(o_{9,12}\text{-CBDT})_6]^{+}$ in their Coulombic adducts for the first time. These results highlight the intrinsic, solvent-independent reactivity of NCs in the gas phase.

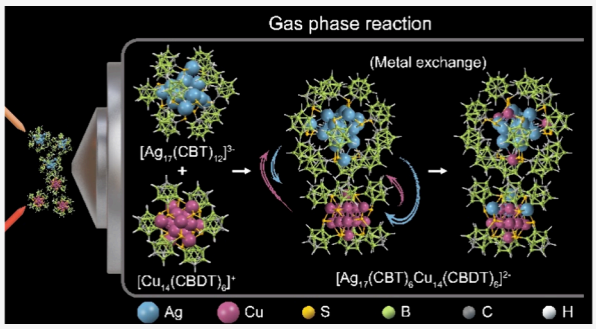

Atomically precise noble metal nanoclusters (NCs) composed of well-defined cores of tens of metal atoms and appropriate ligand shells represent a unique class of materials that form well-defined structures and are now considered to be molecules.[1,2] While their molecular character was inferred early from their optical absorption and photoluminescence properties, it became increasingly evident in later years through their molecular reactivity.[3−7] These NCs have emerged as powerful model systems for probing fundamental processes in nanoscale reactivity, where every atom can be tracked during structural and compositional transformations.[8−18] The reactivity of NCs continues to draw attention, particularly their capacity for atomic exchange with other NCs in solution.[19−22] It was exemplified further using isotopic exchange between NCs, and the thermodynamic and kinetic parameters could be extracted from the reactions.[23] Metal exchange between the NCs often proceeds through transient adduct intermediates, which are rarely isolated due to their short-lived nature.[19,24] In our recent study, we observed a stable NC adduct attributed to the robust metal−ligand interfacial interactions.[25] These studies highlight the remarkable adaptability of NCs and the need to understand their reactivity in detail.

All NC reaction studies thus far have focused on solution-phase reactions, where they undergo dynamic transformations.[26,27] However, it naturally poses a question of the influence of the solvent environment and counterions, which may play an intrinsic role in mediating the process and make it challenging to probe the mechanistic steps involved. The motivation behind the present work was to explore the intercluster reaction in isolation to probe intrinsic intercluster reactivity. As charged species, NCs can form Coulombic adducts driven by electrostatic attraction. Our goal of this study was to investigate what processes occur in a single electrostatic interaction of NCs upon the formation of long-lived gas-phase adducts, revealing their fundamental supramolecular behavior beyond solution chemistry. In solution, atom exchange is initiated by adduct formation mediated by van der Waals, $\pi\cdots\pi$, $\pi\cdots$H−C, dipole−dipole, and metal-

Received: January 9, 2026
Revised: January 27, 2026
Accepted: February 4, 2026

lophilic interactions, which overcome Coulombic repulsion by charge delocalization; however, these interactions are also observed in the gas phase.[24,28−30]

Here, we report Coulombic ion pair formation between two oppositely charged NCs $[Ag_{17}(o_1\text{-CBT})_{12}]^{3-}$ and $[Cu_{14}(o_{9,12}\text{-CBDT})_6]^{+}$ (hereafter referred to as $[Ag_{17}L_{12}]^{3-}$ and $[Cu_{14}L'_6]^{+}$, respectively) in the gas phase, where direct evidence of intercluster atom exchange was captured. Using high-resolution mass spectrometry (HRMS) and tandem mass spectrometry (MS−MS) studies, we observed evidence for Ag-Cu and ligand exchanges within the well-defined Coulombic adducts and the formation of alloy NCs. Complementary density functional theory (DFT) calculations reveal the binding energies (BE) for the ion-pair-driven exchange pathways. This study establishes an ion-pair-mediated, electrostatically driven pathway for atomic exchange, offering new insights into charge-mediated nanocluster reactivity.

Gas-Phase Ion−Ion Reaction between Two NCs. The NCs used in this study, $[Ag_{17}L_{12}]^{3-}$, $[Ag_{29}(1,3\text{-BDT})_{12}]^{3-}$, and $[Cu_{14}L'_6]^{+}$, were synthesized as described in the Experimental section and characterized by nESI-MS (Figure S1). For this reaction, two oppositely charged NCs were introduced via separate capillaries, and the resulting NC ions were isolated in two different trap cells (Q1 and q2) simultaneously. These two ESI emitters were operated sequentially such that the ESI-generated plumes did not interact. The ions from Q1 were then transferred into Q2, where they were simultaneously trapped for ∼600 ms, allowing them to interact and form distinct Coulombic adducts. The opposite polarities of the ions were sequentially generated and transmitted through the instrument to q2. The two polarities were trapped via AC applied to the lenses on either side of q2 for a set amount of time (600 ms). After this time had elapsed, the positive ions were discarded by switching off the AC applied to the lenses and a negative bias was applied to continue trapping the negatively charged precursor and reaction products until they were sent to the TOF mass analyzer. A schematic representation of this process is shown in Figure 1A. In Figure 1B, mass spectra of the isolated NC ions (a) $[Ag_{17}L_{12}]^{3-}$ and (b) $[Cu_{14}L'_6]^{+}$ are shown, where the insets show matching experimental and simulated isotopic distributions, confirming their identities. The distinct Coulombic adducts formed from their interactions are shown in Figure 1C.

When oppositely charged NC ions, $[Ag_{17}L_{12}]^{3-}$ and $[Cu_{14}L'_6]^{+}$, interacted in the gas phase, they rapidly formed Coulombic adducts and related products arising from this electrostatic interaction. Adducts were observed at m/z 3032 ($[Ag_{17}L_{12}Cu_{14}L'_6]^{2-}$) and 8192 ($[Ag_{17}L_{12}(Cu_{14}L'_6)_2]^{-}$), showing charge variation with increasing $[Cu_{14}L'_6]^{+}$ association. Note the change in the charge of the adducts. A third adduct could not be observed, as this would correspond to a neutral species. In addition to these NC-NC adducts, Coulombic adducts of Cu^{+} with $[Ag_{17}L_{12}]^{3-}$ and $[Ag_{17}L_{12}(Cu_{14}L'_6)]^{2-}$ producing $[Ag_{17}L_{12}Cu]^{2-}$ (m/z 2000) and $[Ag_{17}L_{12}(Cu_{14}L'_6)\text{-}Cu]^{-}$ (m/z 6128), respectively, were also detected, as shown in Figure 1(C). The spectrum further showed $[Ag_{17}L_{12}]^{2-}$ at m/z 1968 and $[Ag_{16}L_{10}]^{2-}$ at m/z 1739, indicating electron transfer and fragmentation during the interaction.

Fragmentation of the Coulombic Adducts and Atom Exchanges between the Two NCs Within. We further probed these Coulombic adducts by isolating the first adduct, $[Ag_{17}L_{12}Cu_{14}L'_6]^{2-}$ (Figure 2A), in q2 and subjecting it to resonance ion trap collision-induced dissociation (IT-CID),

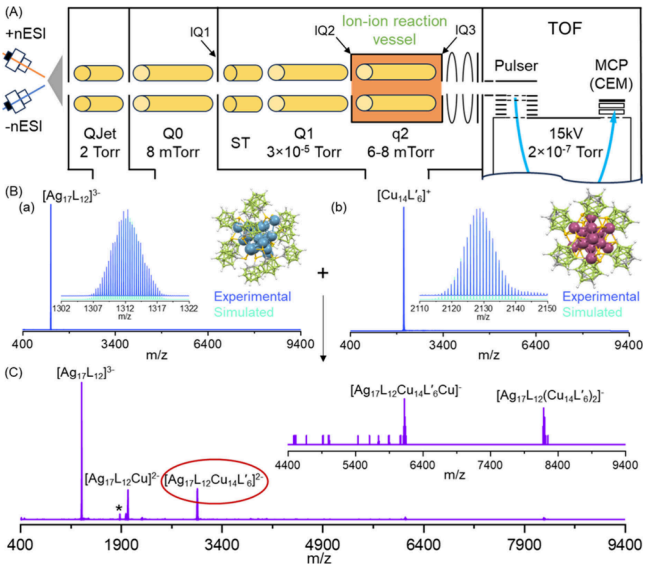

Figure 1. (A) Schematic of the setup for studying gas-phase NC interactions. (B) Mass spectra of isolated NCs (a) $[Ag_{17}L_{12}]^{3-}$ and (b) $[Cu_{14}L'_6]^{+}$, with a comparison of experimental and simulated isotopic distributions and crystal structures in the insets. (C) Mass spectrum of products formed via Coulombic interaction between the two NCs. L = o_1-CBT, L′ = $o_{9,12}$-CBDT, and * = $[Ag_{16}L_{10}]^{2-}$. Color codes for the atoms: blue = Ag, magenta = Cu, yellow = S, green = B, gray = C, and off white = H. The 1:1 Coulombic adduct of the parent clusters is marked with a circle.

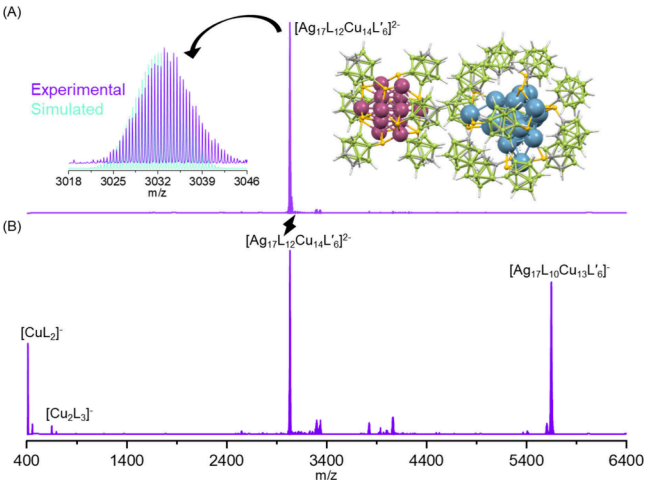

Figure 2. Intramolecular metal exchange. (A) Mass spectrum for the isolated adduct with insets showing a comparison of the experimental and simulated isotopic distributions (left) and DFT-optimized adduct structure (right). (B) MS/MS spectrum showing Ag−Cu exchange via CuL_2 fragments from the Cu-doped Ag_{17} NC. L = o_1-CBT and L′ = $o_{9,12}$-CBDT.

which is shown in Figure 2B. Fragmentation produced complementary species on either side of the precursor: $[Ag_{17}L_{10}Cu_{13}L'_6]^{-}$ at m/z 5650 and $[CuL_2]^{-}$ at m/z 414. There were several other complementary species formed during this fragmentation: $[Ag_{16}L_{10}Cu_{14}L'_6]^{-}$ at m/z 5606 with $[AgL_2]^{-}$ at m/z 458; $[Ag_{17}L_9Cu_{12}L'_6]^{-}$ at m/z 5412 with $[Cu_2L_3]^{-}$ at m/z 652; and $[Ag_{16}L_9(Cu_{13}L'_6)]^{-}$ at m/z 5367 with $[CuAgL_3]^{-}$ at m/z 697. Certain fragment species were observed with a 1− charge that we did not mention initially in the Letter, as we did not observe a complementary peak in the

https://doi.org/10.1021/acs.jpclett.6c00072
J. Phys. Chem. Lett. XXXX, XXX, XXX−XXX

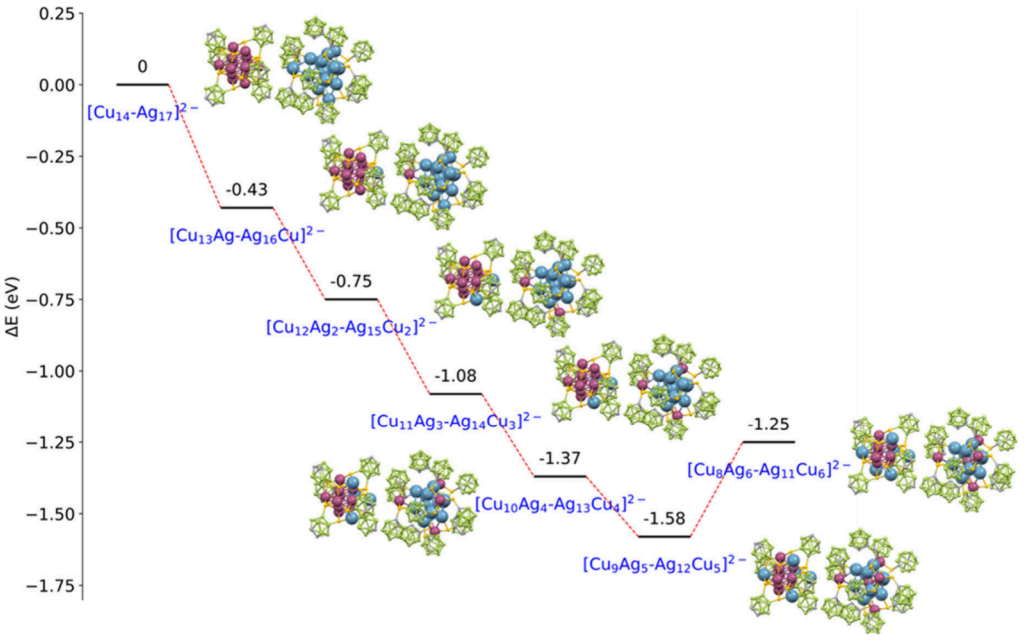

Figure 3. DFT calculation showing a downward trend in reaction energies for one to five sequential Cu−Ag atom exchanges between $[Cu_{14}L'_6]^+$ and $[Ag_{17}L_{12}]^{3-}$ within the adduct.

lower mass. These peaks, however, can be assigned to $[Ag_{13}Cu_4L_{12}Cu]^-$ at m/z 3822, $[Ag_{13}Cu_4L_{10}Cu_2(L'\text{-}S)]^-$ at m/z 3710, $[Ag_{13}Cu_4L_{10}Cu(L'\text{-}S)]^-$ at m/z 3646, $[Ag_{13}Cu_4L_{10}(L'\text{-}S)]^-$ at m/z 3583, $[Ag_{12}Cu_4L_{10}S]^-$ at m/z 3332, and $[Ag_{12}Cu_4L_{10}]^-$ at m/z 3300. These results indicate multiple Cu−Ag exchanges within the adduct, confirming Cu incorporation into Ag_{17} NC. Although the origin of the fragment CuL_2 needs further discussion (see later) (Figure S10), incorporation of Cu into Ag_{17} is evident.

Further gas-phase interaction between $[Ag_{13}Cu_4L_{12}]^{3-}$ and $[Ag_{21}L'_{12}(TPP)_2]^+$ (L′ = m_9-CBT) yielded adducts $[Ag_{13}Cu_4L_{12}Ag_{21}L'_{12}(TPP)]^{2-}$ and $[Ag_{13}Cu_4L_{12}Ag_{21}L'_{12}]^{2-}$, with one and two TPP losses, respectively (Figure S2). Fragmentation of these adducts produced mixed Ag−Cu−L species, confirming metal exchange (Figure S3). Similar Coulombic adduct formation was observed between $[Ag_{22}L_{12}Cl_4(DPPB)_4]^{2+}$ (where L = 2,5-DMBT) and $[Au_{25}L'_{18}]^-$ (where L′ = 2-PET) as shown in Figure S4, and its fragmentation pattern is shown in Figure S5. To establish the generality of this process, gas-phase interactions of $[PdAg_{24}L_{18}]^{2-}$ and $[PtAg_{24}L_{18}]^{2-}$ (where L = 2,4-DMBT) with $[Cu_{14}L'_6]^+$ were also examined (Figures S6 and S7). We also explored the gas-phase interaction of $[PdAg_{28}L_{12}]^{4-}$ and $[PtAg_{28}L_{12}]^{4-}$ (where L = 1,3-BDT) with $[Cu_{14}L'_6]^+$ (Figures S8 and S9), which also confirmed the formation of Coulomb adducts between the NCs.

We performed IT-CID on the parent NCs $[Ag_{17}L_{12}]^{3-}$, $[Ag_{13}Cu_4L_{12}]^{3-}$, and $[Cu_{14}L'_6]^+$ to compare their fragmentation with the adduct $[Ag_{17}L_{12}Cu_{14}L'_6]^{2-}$ (Figure S10). This fragmentation pattern has also been reported in our earlier reports on these NCs.[31,32] The adduct exhibited a pattern similar to that of the parent NCs, losing outermost tetrahedral metal atoms bound to CBT ligands, indicating Cu transfer from Cu_{14} to Ag_{17} within the adduct, specifically only to those staple atoms in the tetrahedral positions. To check the structural stability and equilibrium behavior of adduct $[Ag_{17}L_{12}Cu_{14}L'_6]^{2-}$ in the gas phase, we varied the interaction times of the two NCs in q2 before IT-CID, which showed no change in fragmentation as shown in Figure S11 (within our experimental limits). The geometric confinement and the specific decomposition pathways of the adducts suggest that these kinetically trapped Coulombic adducts do not undergo any further isomerization or that the energy imparted during activation is insufficient to overcome the isomerization barrier.

DFT Modeling of the Coulombic Adducts and Atom Exchanges. We performed DFT calculations to determine the atomistic structure of the adduct and the thermodynamic driving force of the intercluster atom exchanges between $[Ag_{17}L_{12}]^{3-}$ and $[Cu_{14}L'_6]^+$. First, we explored the many configurations of the Coulombic adducts between the two NCs, considering the ligand-shell symmetry of both NCs, like one-to-one, two-to-two, three-to-three, one-to-two, and one-to-three ligand interactions, and identified two stable configurations (Figure S12A,B) whose energies are close and within 0.10 eV (10 kJ/mol). We considered the most stable adduct configuration (Figure S12B), which has a cation−anion BE of 4.62 eV, a closer intercluster metal-to-metal distance of 5.3 Å, and a more compact structure due to the interdigitation of three-to-three ligand interactions for subsequent studies, as also shown in the inset of Figure 2A. By turning off the van der Waals (vdW) interactions in the DFT calculations, the BE decreased to 3.05 eV, indicating that 66% of the total BE is Coulombic and the rest is vdW. We further examined the sequential atom exchanges of Ag and Cu in the adduct and found a downhill trend for 1−5 Cu atoms from $[Cu_{14}L'_6]^+$ exchanged to $[Ag_{17}L_{12}]^{3-}$ in the adduct (Figure 3), indicating a favorable thermodynamic driving force for the metal exchange. First, we started with one Ag−Cu exchange between the two NC ions, with the most feasible positions for exchanged Ag and Cu atoms on the host NC ions which are the outer Cu_8 cubic shell and the outer Ag_4 tetrahedral, respectively (Figure S13). The overall structure of the adduct did not change with atom exchanges. Only individual NC structures changed slightly to accommodate exchanged atoms due to a change in atomic radii. The first four Cu atoms preferentially occupied tetrahedral sites in Ag_{17}, with the fifth replacing the central

https://doi.org/10.1021/acs.jpclett.6c00072
J. Phys. Chem. Lett. XXXX, XXX, XXX−XXX

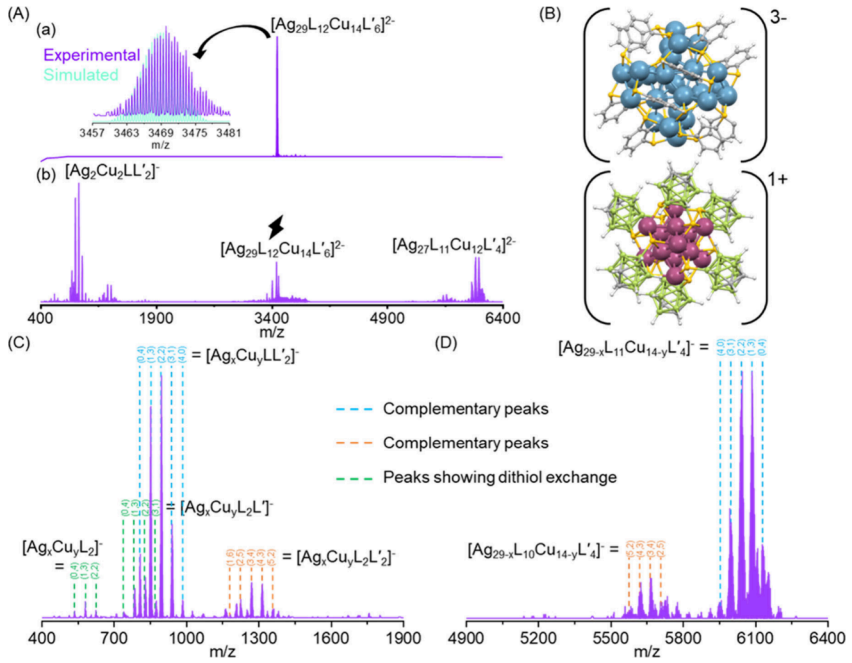

Figure 4. Dithiol exchange between NCs. (A) (a) Mass spectrum of the isolated adduct with an inset showing the simulated vs experimental isotopic distribution. (b) MS/MS spectrum showing sequential Ag−Cu exchanges in the fragmented peaks. (B) Structure of the NCs with their charge states. Detailed Ag−Cu and dithiol exchanges are shown for (C) lower m/z and (D) higher m/z. L = 1,3-BDT and L′ = $o_{9,12}$-CBDT.

Ag atom, while exchanged Ag atoms migrate to the outer Cu_8 shell of Cu_{14}, consistent with four spontaneous Cu exchanges observed in solution (Figure S14). During reaction of $[Ag_{17}(CBT)_{12}]^{3-}$ with $[Cu_{14}(CBDT)_6]^+$ in solution, the immediate exchange of four Cu atoms on $[Ag_{17}(CBT)_{12}]^{3-}$ within 3−5 min was observed, while there were only one to two Ag atom exchanges on the $[Cu_{14}(CBDT)_6]^+$ NC as shown in Figure S14. However, no intercluster adducts were observed during the solution-phase reaction, in contrast to their gas-phase interactions.

Dithiol Exchange between Two NCs in the Isolated State. Similar gas-phase interaction between two dithiol-protected NC ions $[Ag_{29}L_{12}]^{3-}$ (here L= 1,3-BDT) and $[Cu_{14}L'_6]^+$ led to Coulombic adduct $[Ag_{29}L_{12}Cu_{14}L'_6]^{2-}$ (Figure S15). Upon collisional activation, the adduct (Figure 4A(a)) produced complementary fragments, indicating multiple Ag−Cu and dithiol exchanges, as shown in Figure 4A(b). This marks the first observation of dithiol exchange between NCs. Figure 4B shows the molecular structure of NCs $[Ag_{29}L_{12}]^{3-}$ and $[Cu_{14}L'_6]^+$. Expanded spectra of Figure 4A(b) shown in Figure 4C,D of the lower m/z (400−1900) and higher m/z (4900−6400) ranges, respectively, show mixed metal−ligand fragments, unlike the $[Ag_{17}L_{12}Cu_{14}L'_6]^{2-}$ fragmentation. Apparently, the dithiol exchange appears feasible only when both NCs are dithiol-protected. As their solution-phase reaction shows metal but no ligand exchange between $[Ag_{29}L_{12}]^{3-}$ and $[Cu_{14}L'_6]^+$ (Figure S16), this phenomenon appears to be unique to the gas phase.

Apart from this one-on-one adduct, we observed a Cu^+ adduct with $[Ag_{17}(o_1\text{-CBT})_{12}]^{3-}$ and $[Ag_{29}(1,3\text{-BDT})_{12}]^{3-}$. Positive-mode MS of isolated $[Cu_{14}L'_6]^+$ before and during the reaction with the Ag_{17} NC (Figure S17) showed no free Cu^+, indicating its origin from the adduct itself (data in Figure S18). Even after ejecting parent adduct $[Ag_{17}L_{12}Cu_{14}L'_6]^{2-}$ from the collision cell prior to fragmentation, $[Ag_{17}(o_1\text{-CBT})_{12}Cu]^{2-}$ persisted, though its intensity increased with higher oscillation amplitude used for IT-CID (Figure S18), confirming its formation during adduct fragmentation. These Cu^+ adducts also exhibit Cu diffusion into the NC staples, observed during the fragmentation of these adducts in Figures S19 and S20.

In conclusion, atomically precise noble metal nanoclusters (NCs) react in the gas phase by forming Coulombic adducts and subsequently exchange metals to form alloy NCs. The Coulombic contribution accounts for approximately 66% of the total interaction energy of the adduct. This universal behavior of NCs to form Coulombic adducts was observed across multiple NC systems, $[Ag_{17}(o\text{-CBT})_{12}]^{3-}$, $[Ag_{29}(1,3\text{-BDT})_{12}]^{3-}$, $[PdAg_{28}(1,3\text{-BDT})_{12}]^{4-}$, $[PtAg_{28}(1,3\text{-BDT})_{12}]^{4-}$, $[Ag_{13}Cu_4(o_1\text{-CBT})_{12}]^{3-}$, $[Au_{25}(2\text{-PET})_{18}]^-$, $[PdAg_{24}(2,4\text{-DMBT})_{18}]^{2-}$, $[PtAg_{24}(2,4\text{-DMBT})_{18}]^{2-}$, $[Cu_{14}(o_{9,12}\text{-CBDT})_6]^+$, $[Ag_{21}(m_9\text{-CBT})_{12}]^+$, and $[Ag_{22}(2,5\text{-DMBT})_{12}Cl_4(DPPB)_4]^+$, confirming that intercluster reactions arise from intrinsic NC properties, i.e., distributed charges, van der Waals forces, and ligand contacts, rather than solvent effects. The NC ions appear to behave like coordination complexes, which were studied similarly using ion chemistry. These findings establish that atom exchange and supramolecular interactions are inherent to NCs, with gas-phase studies providing direct mechanistic insight complementing solution-phase chemistry.

■ ASSOCIATED CONTENT

Supporting Information

The Supporting Information is available free of charge at https://pubs.acs.org/doi/10.1021/acs.jpclett.6c00072.

Instrumentation, experimental section, MS of parent NCs, detailed MS studies for all of the reactions, detailed MS/MS studies for adducts, and other relevant data (PDF)

Transparent Peer Review report available (PDF)

https://doi.org/10.1021/acs.jpclett.6c00072
J. Phys. Chem. Lett. XXXX, XXX, XXX−XXX

AUTHOR INFORMATION

Corresponding Authors

Tomas Base − *Department of Syntheses, Institute of Inorganic Chemistry, The Czech Academy of Science, Rez 25068, Czech Republic;* orcid.org/0000-0003-2533-8705; Email: tbase@iic.cas.cz

De-en Jiang − *Department of Chemical and Biomolecular Engineering, Vanderbilt University, Nashville, Tennessee 37235, United States;* orcid.org/0000-0001-5167-0731; Email: de-en.jiang@vanderbilt.edu

Scott A. McLuckey − *James Tarpo Jr. and Margaret Tarpo Department of Chemistry, Purdue University, West Lafayette, Indiana 47906-2084, United States;* orcid.org/0000-0002-1648-5570; Email: mcluckey@purdue.edu

Thalappil Pradeep − *DST Unit of Nanoscience (DSTUNS) and Thematic Unit of Excellence (TUE), Department of Chemistry, IIT Madras, Chennai, Tamil Nadu 600036, India;* orcid.org/0000-0003-3174-534X; Email: pradeep@iitm.ac.in

Authors

Swetashree Acharya − *DST Unit of Nanoscience (DSTUNS) and Thematic Unit of Excellence (TUE), Department of Chemistry, IIT Madras, Chennai, Tamil Nadu 600036, India*

Seth Adam Horn − *James Tarpo Jr. and Margaret Tarpo Department of Chemistry, Purdue University, West Lafayette, Indiana 47906-2084, United States*

Vikash Khokhar − *Interdisciplinary Materials Science, Vanderbilt University, Nashville, Tennessee 37235, United States*

Nicolas J. Pizzala − *James Tarpo Jr. and Margaret Tarpo Department of Chemistry, Purdue University, West Lafayette, Indiana 47906-2084, United States*

Vivek Yadav − *DST Unit of Nanoscience (DSTUNS) and Thematic Unit of Excellence (TUE), Department of Chemistry, IIT Madras, Chennai, Tamil Nadu 600036, India;* orcid.org/0009-0004-0244-0541

Subrata Duary − *DST Unit of Nanoscience (DSTUNS) and Thematic Unit of Excellence (TUE), Department of Chemistry, IIT Madras, Chennai, Tamil Nadu 600036, India*

Complete contact information is available at: https://pubs.acs.org/10.1021/acs.jpclett.6c00072

Notes

The authors declare no competing financial interest.

ACKNOWLEDGMENTS

S.A., V.Y., and S.D. acknowledge support from the Prime Minister's Research Fellowship (PMRF). T.P. acknowledges funding through the Centre of Excellence (CoE) on Molecular Materials and Functions, under the Institute of Eminence Program, the Science and Engineering Research Board (SERB), India (SPR/2021/000439), and a JC Bose Fellowship. S.A. also thanks IIE for funding the research visit. DFT computation was supported by the U.S. Department of Energy, Office of Science, Office of Basic Energy Sciences, Chemical Sciences, Geosciences, and Biosciences Division, Catalysis Science Program. S.A.H. and S.A.M. acknowledge support from the U.S. National Science Foundation under grant CHE-2304386.

REFERENCES

(1) Chakraborty, I.; Pradeep, T. Atomically Precise Clusters of Noble Metals: Emerging Link between Atoms and Nanoparticles. *Chem. Rev.* **2017**, *117* (12), 8208−8271.

(2) Jin, R.; Zeng, C.; Zhou, M.; Chen, Y. Atomically Precise Colloidal Metal Nanoclusters and Nanoparticles: Fundamentals and Opportunities. *Chem. Rev.* **2016**, *116* (18), 10346−10413.

(3) Jin, R. Atomically Precise Metal Nanoclusters: Stable Sizes and Optical Properties. *Nanoscale* **2015**, *7* (5), 1549−1565.

(4) Yao, Q.; Wu, Z.; Liu, Z.; Lin, Y.; Yuan, X.; Xie, J. Molecular Reactivity of Thiolate-Protected Noble Metal Nanoclusters: Synthesis, Self-Assembly, and Applications. *Chem. Sci.* **2021**, *12* (1), 99−127.

(5) Som, A.; Samal, A. K.; Udayabhaskararao, T.; Bootharaju, M. S.; Pradeep, T. Manifestation of the Difference in Reactivity of Silver Clusters in Contrast to Its Ions and Nanoparticles: The Growth of Metal Tipped Te Nanowires. *Chem. Mater.* **2014**, *26* (10), 3049−3056.

(6) Zhong, Y.; Wu, Z.; Bai, X.; Zhang, Y.; Xie, J. Viewing Inorganic Metal Nanoclusters through the Lens of Molecular Chemistry. *Mater. Today* **2024**, *76*, 72−93.

(7) Qian, J.; Yang, Z.; Lyu, J.; Yao, Q.; Xie, J. Molecular Interactions in Atomically Precise Metal Nanoclusters. *Precision Chemistry* **2024**, *2* (10), 495−517.

(8) Zheng, K.; Fung, V.; Yuan, X.; Jiang, D.; Xie, J. Real Time Monitoring of the Dynamic Intracluster Diffusion of Single Gold Atoms into Silver Nanoclusters. *J. Am. Chem. Soc.* **2019**, *141* (48), 18977−18983.

(9) Cao, Y.; Fung, V.; Yao, Q.; Chen, T.; Zang, S.; Jiang, D.; Xie, J. Control of Single-Ligand Chemistry on Thiolated Au25 Nanoclusters. *Nat. Commun.* **2020**, *11* (1), 5498.

(10) Roy, J.; Das, A.; Jana, A.; Chakraborty, P.; Neumaier, M.; Hahn, H.; Pathak, B.; Kappes, M. M.; Pradeep, T. Structural Changes in Atomically Precise Ag29 Nanoclusters upon Sequential Attachment and Detachment of Secondary Ligands. *ACS Nano* **2025**, *19* (5), 5727−5738.

(11) Chakraborty, P.; Neumaier, M.; Seibel, J.; Da Roit, N.; Böttcher, A.; Schmitt, C.; Wang, D.; Kübel, C.; Behrens, S.; Kappes, M. M. Exploring the Activation of Atomically Precise [Pt17(CO)12(PPh3)8]2+ Clusters: Mechanism and Energetics in Gas Phase and on an Inert Surface. *ACS Nano* **2025**, *19* (3), 3624−3634.

(12) Negishi, Y.; Munakata, K.; Ohgake, W.; Nobusada, K. Effect of Copper Doping on Electronic Structure, Geometric Structure, and Stability of Thiolate-Protected Au25 Nanoclusters. *J. Phys. Chem. Lett.* **2012**, *3* (16), 2209−2214.

(13) Buschmann, D. A.; Hirai, H.; Tsukuda, T. Tuning Photoluminescence Properties of Au Clusters by Surface Modification and Doping: Lessons from Case Studies of Icosahedral Au 13. *Inorganic Chemistry Frontiers* **2024**, *11* (20), 6694−6710.

(14) Wang, S.; Han, C.; Chen, X.; Xiang, Y.; Li, Q.; Chai, J.; Yang, S.; Du, Y.; Luo, Q.; Zhu, M. Constructing Atomic-Level Defect as the Catalytic Site by Removing a Single Metal Atom from the Nanoclusters. *ACS Nano* **2025**, *19* (27), 25334−25341.

(15) Zhu, C.; Li, F.; Xia, J.; Shi, Z.; Yu, M.; Dong, W.; Li, S.; Hu, Z.; Wu, Z.; Kang, X.; Zhu, M. Single-Site Metal-Nonmetal Microenvironment Regulation of Copper Nanoclusters with Atomic Precision for X-Ray Imaging. *Angew. Chem., Int. Ed.* **2025**, *64* (38), No. e202511261.

(16) Chiu, T.-H.; Pillay, M. N.; Wu, Y.-Y.; Niihori, Y.; Negishi, Y.; Chen, J.-Y.; Chen, Y. J.; Kahlal, S.; Saillard, J.-Y.; Liu, C. W. Controlled Aggregation of Pt/PtH/Rh/RhH Doped Silver Superatomic Nanoclusters into 16-Electron Supermolecules. *Chemical Science* **2024**, *15* (36), 14660−14667.

(17) Niihori, Y.; Eguro, M.; Kato, A.; Sharma, S.; Kumar, B.; Kurashige, W.; Nobusada, K.; Negishi, Y. Improvements in the Ligand-Exchange Reactivity of Phenylethanethiolate-Protected Au25 Nanocluster by Ag or Cu Incorporation. *J. Phys. Chem. C* **2016**, *120* (26), 14301−14309.

(18) Jana, A.; Dar, W. A.; Jana, S. K.; Poonia, A. K.; Yadav, V.; Roy, J.; Chandra, S.; Adarsh, K. N. V. D.; Ras, R. H. A.; Pradeep, T. Photoconversion of Ag31 to Ag42 Initiated by Solvated Electrons. *Chem. Mater.* **2023**, *35* (17), 7020−7031.
(19) Krishnadas, K. R.; Baksi, A.; Ghosh, A.; Natarajan, G.; Pradeep, T. Structure-Conserving Spontaneous Transformations between Nanoparticles. *Nat. Commun.* **2016**, *7* (1), 13447.
(20) Krishnadas, K. R.; Ghosh, A.; Baksi, A.; Chakraborty, I.; Natarajan, G.; Pradeep, T. Intercluster Reactions between $Au_{25}(SR)_{18}$ and $Ag_{44}(SR)_{30}$. *J. Am. Chem. Soc.* **2016**, *138* (1), 140−148.
(21) Ghosh, A.; Ghosh, D.; Khatun, E.; Chakraborty, P.; Pradeep, T. Unusual Reactivity of Dithiol Protected Clusters in Comparison to Monothiol Protected Clusters: Studies Using $Ag_{51}(BDT)_{19}(TPP)_3$ and $Ag_{29}(BDT)_{12}(TPP)_4$. *Nanoscale* **2017**, *9* (3), 1068−1077.
(22) Khatun, E.; Chakraborty, P.; Jacob, B. R.; Paramasivam, G.; Bodiuzzaman, M.; Dar, W. A.; Pradeep, T. Intercluster Reactions Resulting in Silver-Rich Trimetallic Nanoclusters. *Chem. Mater.* **2020**, *32* (1), 611−619.
(23) Chakraborty, P.; Nag, A.; Natarajan, G.; Bandyopadhyay, N.; Paramasivam, G.; Panwar, M. K.; Chakrabarti, J.; Pradeep, T. Rapid Isotopic Exchange in Nanoparticles. *Science Advances* **2019**, *5* (1), No. eaau7555.
(24) Neumaier, M.; Baksi, A.; Weis, P.; Schneider, E. K.; Chakraborty, P.; Hahn, H.; Pradeep, T.; Kappes, M. M. Kinetics of Intercluster Reactions between Atomically Precise Noble Metal Clusters [Ag25(DMBT)18]− and [Au25(PET)18]− in Room Temperature Solutions. *J. Am. Chem. Soc.* **2021**, *143* (18), 6969−6980.
(25) Acharya, S.; Roy, J.; Roy, D.; Pathak, B.; Pradeep, T. Stable Dimer Intermediates during Intercluster Reactions of Atomically Precise Nanoclusters. *J. Phys. Chem. C* **2025**, *129*, 5840.
(26) Bose, P.; Ramankutty, K. K.; Chakraborty, P.; Khatun, E.; Pradeep, T. A Concise Guide to Chemical Reactions of Atomically Precise Noble Metal Nanoclusters. *Nanoscale* **2024**, *16* (4), 1446−1470.
(27) Gratious, S.; Li, B.; Mondal, D.; Kumar, A.; Aleyamma Varghese, D.; Thomas, J.; Jiang, D.; Kamble, V.; Mandal, S. Identifying the Superatomic AuCu 56 Nanocluster through a Ligand-Exchange Coupled Metal-Exchange Induced Transformation. *Chemical Science* **2025**, *16* (26), 11849−11857.
(28) Chandrashekar, P.; Varghese, D. A.; Thomas, T.; Pal, A. K.; Muraleedharan, A.; Salam, A.; Ghosh, M.; Mondal, P. K.; Suresh, S. V.; Nandi, C. K.; Datta, A.; Mandal, S. Two- and Three-Dimensional Silver Cluster Assemblies: Effect of Argentophilic Interactions in Photoluminescence. *J. Phys. Chem. Lett.* **2025**, *16* (16), 4107−4113.
(29) Shingyouchi, Y.; Ogami, M.; Biswas, S.; Tanaka, T.; Kamiyama, M.; Ikeda, K.; Hossain, S.; Yoshigoe, Y.; Osborn, D. J.; Metha, G. F.; Kawawaki, T.; Negishi, Y. Ligand-Dependent Intracluster Interactions in Electrochemical CO2 Reduction Using Cu14 Nanoclusters. *Small* **2025**, *21* (16), 2409910.
(30) Nakashima, Y.; Ito, S.; Koyasu, K.; Tsukuda, T. Formation of Dimers of [MAu24(SCnH2n+1)18]− (M = Au, Pt; n = 6, 8, 10, 12) in Gas Phase by Overcoming Electrostatic Repulsion through Aurophilic and Multiple vdW Attractions. *J. Phys. Chem. Lett.* **2025**, *16* (27), 6954−6959.
(31) Yadav, V.; Jana, A.; Acharya, S.; Malola, S.; Nagar, H.; Sharma, A.; Kini, A. R.; Antharjanam, S.; Machacek, J.; Adarsh, K. N. V. D.; Base, T.; Häkkinen, H.; Pradeep, T. Site-Specific Substitution in Atomically Precise Carboranethiol-Protected Nanoclusters and Concomitant Changes in Electronic Properties. *Nat. Commun.* **2025**, *16* (1), 1197.
(32) Jana, A.; Duary, S.; Das, A.; Kini, A. R.; Acharya, S.; Machacek, J.; Pathak, B.; Base, T.; Pradeep, T. Multicolor Photoluminescence of Cu14 Clusters Modulated Using Surface Ligands. *Chem. Sci.* **2024**, *15* (34), 13741−13752.

https://doi.org/10.1021/acs.jpclett.6c00072
J. Phys. Chem. Lett. XXXX, XXX, XXX−XXX